Published by IOP Publishing for Sissa Medialab

Received: *September 24, 2019*
Revised: *December 17, 2019*
Accepted: *January 17, 2020*
Published: *February 6, 2020*

2020 JINST 15 P02002

Improvement in sensitivity of an indirect-type organic X-ray detector using an amorphous IGZO interfacial layer

H. Liu,[a] **S. Hussain**[b] **and J. Kang**[a,1]

[a] *Department of Electronics and Electrical Engineering, Dankook University, 152, Jukjeon-ro, Suji-gu, Yongin-si, Gyeonggi-do, 16890, Republic of Korea*
[b] *Department of Nano and Advanced Materials Engineering, Sejong University, 209, Neungdong-ro, Gwangjin-gu, Seoul, 05006, Republic of Korea*

E-mail: jkang@dankook.ac.kr

Abstract: To improve the power conversion efficiency (PCE) and sensitivity of indirect-type organic X-ray detectors, we examined the role of amorphous indium-gallium-zinc-oxide (a-IGZO) as an interfacial layer placed between the PBDB-T: PCBM active layer and the LiF/Al cathode. By RF magnetron sputtering, a-IGZO films with different thicknesses were deposited on a PBDB-T: PCBM active layer at room temperature. The optimized detector with a 10.1 nm a-IGZO layer achieved the highest PCE of 7.45% under artificial solar illumination, which was higher than the PCE (5.43%) of the detector without an a-IGZO layer. Furthermore, the highest sensitivity of 2.82 mA/Gy·cm^2 under X-ray exposure was achieved for the detector with the 10.1 nm a-IGZO layer, which was an improvement of 26% over the X-ray detector without an a-IGZO layer.

Keywords: Materials for solid-state detectors; Photon detectors for UV, visible and IR photons (solid-state); Solid state detectors; Scintillators, scintillation and light emission processes (solid, gas and liquid scintillators)

[1]Corresponding author.

https://doi.org/10.1088/1748-0221/15/02/P02002

Contents

2020 JINST 15 P02002

1 Introduction

Organic polymers based on a solution process with bulk heterojunctions (BHJs) have been employed to fabricate light-emitting diodes, photovoltaic devices, and optical sensors. Moreover, organic-based BHJ detectors are receiving much attention for medical X-ray detection in both the academic and industrial fields because of their advantages, such as low cost, diversity of molecular designs, light weight, solution-based processes, and morphological stability caused by the entanglement of polymers, large-area capability, and the ability to fabricate curved imagers. Many methods have been proposed for the use of organic polymers in X-ray detectors based on a solution process. Given their excellent photon absorption, photon-to-charge conversion efficiency, and charge-carrier transport, two types of organic detectors for medical X-ray detection have been developed and classified into scintillator-coupled indirect detectors [1, 2] and photoconductor-coupled direct detectors [3, 4]. In scintillator-coupled indirect detectors, the incident X-rays are converted into visible light through the scintillator, and charge-carriers are generated in the active layer by incoming visible light, whereas in photoconductor-coupled direct detectors, the incident X-rays are converted directly to charge-carriers in the active layer of the detector.

Although various research groups have applied conjugated polymer poly (3-hexylthiophene) (P3HT) as a p-type semiconductor and fullerene derivative phenyl-C61-butyric acid methyl ester (PCBM) as an n-type semiconductor to form an active layer for organic detectors, the applied detectors showed inferior detection sensitivity. The device is also unstable because of the poor morphology of the applied organic layer and its susceptibility to oxygen and moisture. Recently, the photon-to-charge conversion efficiency of organic BHJ devices, including X-ray detectors, have been improved in various ways, such as by applying new low band-gap polymers [5], optimized nano-morphology [6], and additional charge-transporting materials, such as CdSe quantum dots [7] and TiN nanoparticles [8]. In addition, electron- and hole-transport layers added to the organic BHJ active layer improved the photon-generating carrier transport. Polar solvent [9] and WO_3

nanoparticles [10] have been applied to the hole-transport layer and V_2O_5 nanoparticles [11] and small organic molecules (ITCPTC) [12] have been added to the electron-transport layer.

In this work, we applied an organic polymer/fullerene blended layer of poly [5,7-Bis(2-Ethylhexyl) benzo [1,2-c: 4,5-c′] dithiophene-4,8-dione]: [6,6]-phenylC71-butyric acid methyl ester (PBDB-T: PCBM) to study the relationship between detector performance and interfacial properties. The PBDB-T: PCBM active layer has received considerable attention because of its high conversion efficiency [13]. We applied a transparent amorphous indium-gallium-zinc-oxide (a-IGZO) film with different thicknesses as an interfacial layer, which improved the sensitivity of the indirect X-ray detector with a PBDB-T: PCBM layer. We measured current density-voltage (J-V) characteristics during artificial solar and X-ray exposure to evaluate the basic properties of the proposed detector.

2 Experimental preparations

2.1 Fabrication of the detector

Figure 1(a) shows the energy-band diagram of the proposed detector with a PBDB-T: PCBM active layer. The detector consisted of a glass substrate, an ITO anode, poly (3,4-ethylene dioxythiophene): poly(styrene sulfonate) (PEDOT: PSS) as a hole transport layer (HTL), a PBDB-T: PCBM active layer, a-IGZO as an electron transport layer (ETL), and a LiF/Al cathode. The proposed detector was combined with CsI (Tl) scintillators to convert incident X-ray photons into visible photons. The procedure for fabricating the detector is shown in figure 1(b). First, we cleaned the ITO-patterned glass by consecutive treatment with acetone, methanol, and isopropyl alcohol, then dried it in a vacuum oven at 120°C. A PEDOT: PSS layer with a thickness of 40 nm was spin-coated onto the cleaned ITO substrate at 3000 rpm for 30 s and then annealed at 150°C for 30 min. A 2:3 mixture of PBDB-T and PCBM obtained from the previous study [13] was completely dissolved in chlorobenzene at a concentration of 20 mg/ml. Subsequently, the active layer was spin-coated onto the PEDOT: PSS layer at 1100 rpm for 30 s. We then treated the film by thermal annealing at 150°C for 10 min. To block hole transport and improve electron transport from the active layer, a-IGZO thin films grown under different process times, such as 5.9 nm for 4 min, 10.1 nm for 6 min, and 13.8 nm for 8 min, were deposited onto the surface of the active layer at room temperature by radio-frequency (RF) magnetron sputtering. A circular a-IGZO target consisting of In : Ga : Zn = 1 : 1 : 1 was used. The RF power was 50 W, the pressure was 3×10^{-6} torr, and the Ar flow-rate was kept constant at 20 sccm. Contrary to the previous results [13], a time delay occurred between the active layer formation and the cathode formation because RF sputtering equipment located outside the laboratory was used to form the a-IGZO layer. Layers of 5-nm thick LiF and 120-nm thick Al were deposited onto the a-IGZO ETL by thermal evaporation under a pressure of 3×10^{-7} torr. Four cells with an effective area of 4 mm^2 were formed on the X-ray detector. To prevent the fabricated detector from being exposed to oxygen and moisture, it was encapsulated in a glass cover in a glovebox. Finally, a CsI(Tl) scintillator (Hamamatsu J13113) was connected to the glass substrate with an optical adhesive.

2020 JINST 15 P02002

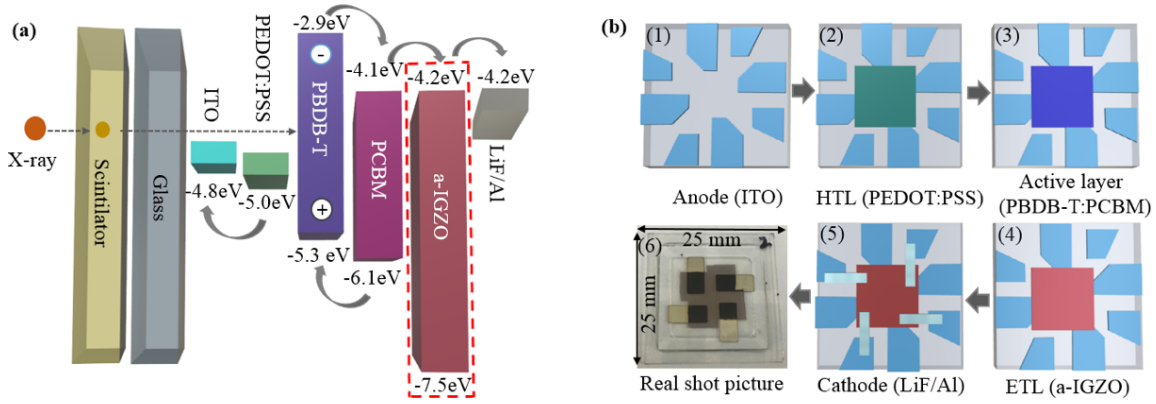

Figure 1. (a) Energy-band diagram of the proposed detector with a-IGZO ETL and (b) process flow of the proposed detector.

2.2 Characterization methods

We characterized the crystallinity of the IGZO thin films by in-plane X-ray diffraction (XRD, Rigaku D/Max-2500) with Cu-Kα radiation operated at 50 kV and 300 mA. Field-emission scanning electron microscopy (FE-SEM, Hitachi S-4700) was used to examine the crosssection of the fabricated detector. We investigated the morphology and roughness of the samples using atomic force microscopy (AFM, Veeco Dimension 3100). Transmittance spectra of the stacked thin films were obtained using a UV−vis spectrophotometer (Optizen 2120UV). We measured the emission spectrum of the CsI(Tl) scintillator (Hamamatsu Photonics J1311) under X-ray irradiation with a spectrometer (AvaSpec ULS2048L) and the current density-voltage (J−V) characteristics of the scintillator-separated detector with an electrometer (Keithley 6571B) under the exposure of an AM 1.5G-filtered Xe lamp with an intensity of 100 mW/cm^2. We also measured the J-V characteristics of the scintillator-coupled detector while it was exposed to an X-ray generator (AJEX 2000H). The exposed X-ray dose was measured using an ion chamber (Capintec CII50).

3 Results and discussion

3.1 Physical properties of the stacked thin films including an a-IGZO layer

FE-SEM analysis was used to study the cross-sectional status of the deposited a-IGZO film on the glass/ITO/PBDB-T: PCBM stacked structure. Figure 2(a) shows the cross-sectional FE-SEM image for the glass/ITO/PBDB-T: PCBM/a-IGZO. The FE-SEM image confirmed that an a-IGZO film was successfully formed on the PBDB-T: PCBM active layer. Figure 2(b) shows the XRD patterns of a-IGZO thin films with different thicknesses. No crystalline peaks were observed in the XRD patterns of any of the IGZO films grown at room temperature. The applied IGZO film had an amorphous phase with other organic materials, which is advantageous in terms of flexible detector implementation and radiation damage.

We used AFM analysis to demonstrate the topological variations of the prepared samples. Figure 3 shows the topographical 3D images of the a-IGZO (10.1 nm), PBDB-T: PCBM (91.2 nm), and PBDB-T: PCBM/a-IGZO samples. All samples were prepared on ITO-coated glass substrates.

2020 JINST 15 P02002

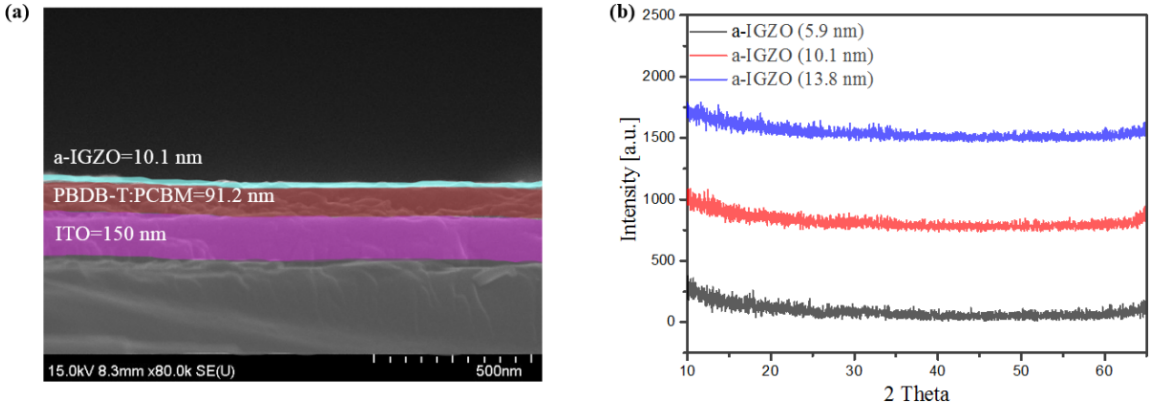

Figure 2. (a) Cross-sectional FE-SEM image of glass/ITO/PBDB-T: PCBM/a-IGZO (10.1 nm) and (b) XRD patterns of RF sputtered IGZO thin films.

As shown in figure 3(a), a highly strained topological property was observed for the a-IGZO sample. We observed homogeneous topology for the PBDB-T: PCBM sample in figure 3(b) and the lowest surface roughness in the PBDB-T: PCBM/a-IGZO sample in figure 3(c). As the surface roughness decreased, the resistance of the device tended to decrease. Therefore, the application of an a-IGZO layer was necessary to improve the electrical properties of the detector.

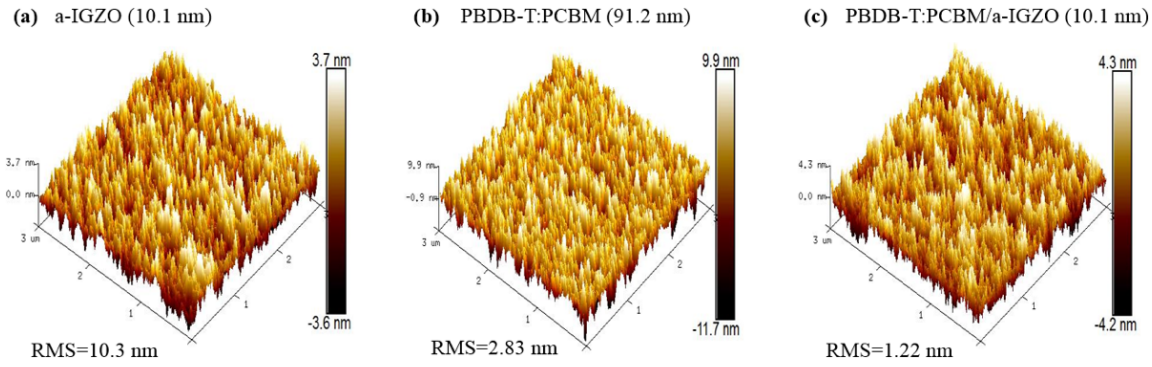

Figure 3. Topographical AFM 3D views of the samples.

Since the indirect-type detector uses visible light generated from a scintillator, a high transmission property of the detector is important. Figure 4 shows the transmittance curves in the visible region with or without a-IGZO films coated on the PBDB-T: PCBM substrates. We measured the transmittance curves by using a UV-Vis spectrophotometer. Because of the surface roughness effect of a-IGZO, the transmittance of the sample increased significantly after the deposition of an a-IGZO layer on the glass/ITO/PBDB-T: PCBM substrates. The emission spectrum of the CsI(Tl) scintillator (red line) in figure 4 shows a maximum emission at 550 nm. When a-IGZO was applied, the transmittance increased by more than 15% in the vicinity of 550 nm compared to the absence of an a-IGZO layer. The highest transmittance was obtained when 10.1 nm a-IGZO was deposited.

2020 JINST 15 P02002

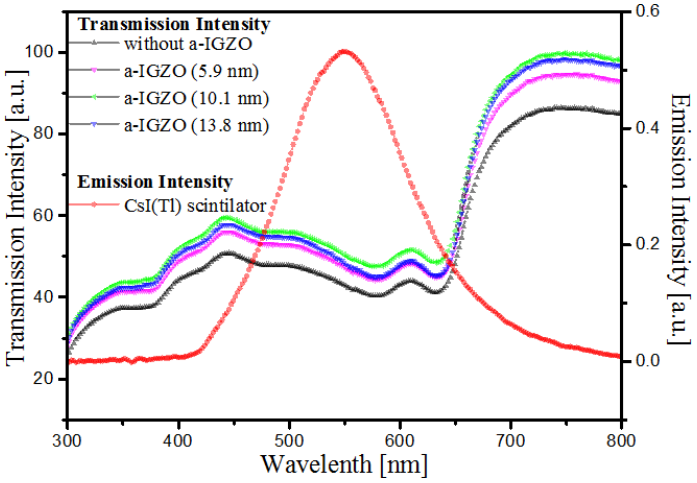

Figure 4. Transmission spectra of the samples and emission spectrum of the CsI(Tl) scintillator.

3.2 Change in detector performance with an a-IGZO layer

To understand the interfacial effect of the a-IGZO layer on detector performance, we measured current density-voltage (J-V) characteristics using an electrometer under illuminations by a solar simulator (San Ei XES40S2-CE). The detector without the scintillator was exposed to an AM 1.5G-filtered Xe lamp in the simulator and the structure of the proposed detector is schematically provided in figure 5. Bias from −1.0 V to 1.0 V was applied to the detector for the charge collection. The detector fabricated without an a-IGZO film showed that the short-circuit current density (J_{SC}) at a bias of 0 V was 11.56 mA/cm^2 and the power conversion efficiency (PCE) related to the photon-to-charge conversion efficiency was 5.43%. After an a-IGZO thin film was applied between the active layer and the metal cathode, the photoelectric performance of the detector was improved remarkably. The detector fabricated with a 10.1 nm a-IGZO layer showed the highest J_{SC} and highest PCE, which were 13.75 mA/cm^2 and 7.45%, respectively. Compared to the detector without an a-IGZO layer, the PCE improved by 37%. Moreover, we observed better PCEs for the detectors with 5.9 nm and 13.8 nm a-IGZO layers, which were 6.86% and 6.58%, respectively. As the a-IGZO film thickness increased, the series resistance of the detector tended to increase and when the a-IGZO film became too thin, an uneven morphology resulted. In both cases, the J_{SC} and PCE were lower than in the detector with a 10.1 nm a-IGZO layer because the charge transport was inhibited. After incorporation of an a-IGZO layer onto the PBDB-T:PCBM active layer, the light-absorption capacity of the detector improved over that of the detector without an a-IGZO layer, which could have stimulated the exciton generation. In addition, moderately thick a-IGZO provided powerful percolation networks for charge transport and collection, which improved the electron mobility and increased the J_{SC}.

Figure 6(a) shows the logarithmic J-V characteristics of the detectors without and with a-IGZO layers grown for different process times. By curve-fitting the logarithmic J−V characteristics, carrier mobility can be obtained using the modified Mott-Gurney equation, as follows:

$$J = \frac{9}{8}\varepsilon_r \varepsilon_o \mu \frac{V^2}{L^3}$$

2020 JINST 15 P02002

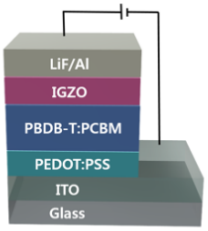

Device	Jsc [mA/cm^2]	PCE [%]	Rs [Ω]
without a-IGZO	11.56 ± 0.05	5.43 ± 0.02	318.78 ± 5.1
a-IGZO (5.9 nm)	12.98 ± 0.01	6.86 ± 0.08	153.53 ± 4.3
a-IGZO (10.1 nm)	13.75 ± 0.09	7.45 ± 0.01	138.56 ± 3.5
a-IGZO (13.8 nm)	12.22 ± 0.07	6.58 ± 0.07	224.34 ± 4.6

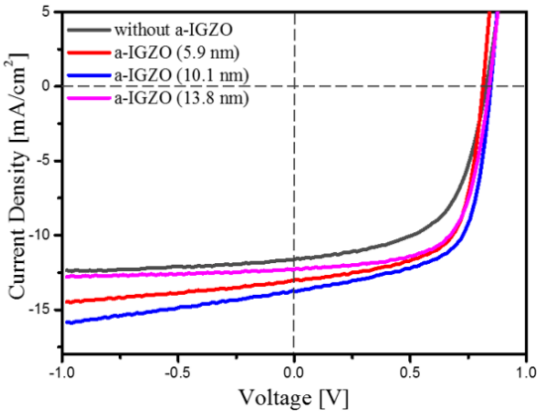

Figure 5. Schematic diagram of the proposed detector without the CsI(Tl) scintillator and J-V characteristics of the detector.

where ε_o (8.85×10^{14} F/cm) is the permittivity of the free space, ε_r is the relative dielectric constant of the active layer, μ is the carrier mobility, V is the voltage drop across the detector, and L is the thickness of the active layer. We calculated the μ values in the space-charge limited current (SCLC) region in the dark [14]. The calculated carrier mobility of the detectors was 3.82×10^{-5} cm^2/V·s for the detector without an a-IGZO layer and 3.12×10^{-4}, 5.44×10^{-4}, and 1.23×10^{-4} cm^2/V·s for the detectors with 5.9 nm, 10.1 nm and 13.8 nm a-IGZO layers, respectively. Mobility was increased by the incorporation of an a-IGZO layer onto the PBDB-T: PCBM active layer. In addition to the increased transmittance from the application of an a-IGZO layer, the reduction in surface roughness and interfacial defects improved the electron transport pathways.

As shown in figure 6(b), the radiation parameters during X-ray exposure, such as collected charge density (CCD) and the sensitivity of the detector, were calculated based on the number of collected charges. The average values obtained from four detectors were presented. The sensitivity was calculated using the following equation:

$$\text{Sensitivity}\left[\frac{\text{mA}}{\text{Gy}\cdot\text{cm}^2}\right] = \frac{\int C(t)_{\text{X-rayon}}\,dt - \int C(t)_{\text{X-rayoff}}\,dt}{\text{Exposure Time}\cdot\text{Absorbed Dose}\cdot\text{Detection Area}}$$

The operation conditions of the X-ray generator were fixed at 80 kVp and 63 mAs and the exposure time was 1.57 s for all of the experiments. The absorbed dose was converted from the exposure, which was measured using an ion chamber. The X-ray detector prepared without an a-IGZO layer showed a sensitivity of 2.23 mA/Gy·cm^2 and a CCD of 289.66 nA/cm^2. The X-ray detector with a 10.1 nm a-IGZO layer showed the highest sensitivity and CCD, which were 2.82 mA/Gy·cm^2 and 391.35 nA/cm^2, respectively. The sensitivity was improved by 26% over that of the X-ray detector fabricated without an a-IGZO layer. Improving the transmittance and surface roughness of the detector by applying an a-IGZO layer improved the detection sensitivity. The sensitivity and CCD values were extracted from the 3rd quadrant of the J-V curves of the scintillator-coupled detectors under X-ray exposure. Therefore, these radiation parameters were highly dependent on the J_{SC} and PCE calculated from the 4th quadrant of the J-V curves of the scintillator-decoupled detector under artificial solar exposure.

2020 JINST 15 P02002

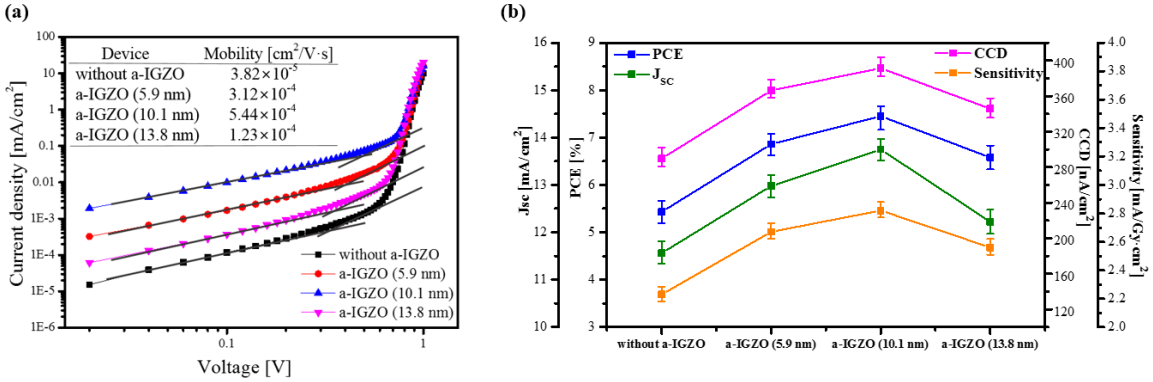

Figure 6. (a) Current density-voltage behavior in the dark and (b) Jsc, PCE, CCD, and sensitivity of the detector without and with an a-IGZO layer.

4 Conclusion

In this work, we investigated the role of an a-IGZO interfacial layer between the PBDB-T: PCBM active layer and the LiF/Al cathode for indirect-type X-ray detector. Applying an a-IGZO layer improved the transmittance of the detector about 15% in the vicinity of 550 nm, which could stimulate carrier-generation. The surface roughness was reduced by applying an a-IGZO layer, which provided powerful percolation paths for carrier transport. The highest PCE of 7.4% was achieved for the detector prepared with a 10.1 nm a-IGZO layer under artificial solar illumination and it was higher than the PCE (5.4%) of the detector without an a-IGZO layer. In addition, the detector with a 10.1 nm a-IGZO layer showed the highest sensitivity of 2.82 mA/Gy·cm^2 and the highest CCD of 391.35 nA/cm^2 under X-ray exposure. This sensitivity was improved by 26% over that of the detector without an a-IGZO layer. The application of an a-IGZO interfacial layer improved the optical and electrical properties of the detector. Therefore, the incorporation of an a-IGZO layer could play a crucial role in improving the performance of organic X-ray detectors.

Acknowledgments

This work was supported by the National Research Foundation of Korea (NRF) grant funded by the Korean government (MSIT) (No. NRF-2017R1A2A2A05069821).

References

[1] P. Büchele et al., *X-ray imaging with scintillator-sensitized hybrid organic photodetectors*, *Nat. Photonics.* **9** (2015) 843.

[2] J. Lee et al., *Comparative studies between photovoltaic and radiation parameters in indirect-type organic X-ray detector with a P3HT: PCBM active layer*, *Nanosci. Nanotech. Lett.* **9** (2017) 1159.

[3] L. Basiricò et al., *Direct X-ray photoconversion in flexible organic thin film devices operated below 1 V*, *Nat. Commun.* **7** (2016) 13063.

[4] D.M. Panneerselvam et al., *Evaluation of organic perovskite photoconductors for direct conversion X-ray imaging detectors*, *J. Mater. Sci. Mater. Electron.* **28** (2017) 7083.

2020 JINST 15 P02002

[5] T. Ameri et al., *Performance Enhancement of the P3HT/PCBM Solar Cells through NIR Sensitization Using a Small-Bandgap Polymer*, *Adv. Energy Mater.* **2** (2012) 1198.

[6] S. Guo et al., *The Effect of Fluorination in Manipulating the Nanomorphology in PTB7: $PC_{71}BM$ Bulk Heterojunction Systems*, *Adv. Energy Mater.* **5** (2015) 1401315.

[7] B. Kim et al., *Improving the sensitivity of indirect-type organic X-ray detector by blending with CdSe quantum dots*, 2017 *JINST* **12** C01009.

[8] A.A. Hussain et al., *Self-powered broadband photodetector using plasmonic titanium nitride*, *ACS Appl. Mater. Interfaces* **8** (2016) 4258.

[9] D. Huang et al., *Perovskite solar cells with a DMSO-treated PEDOT: PSS hole transport layer exhibit higher photovoltaic performance and enhanced durability*, *Nanoscale* **9** (2017) 4236.

[10] T. Stubhan et al., *High fill factor polymer solar cells incorporating a low temperature solution processed WO3 hole extraction layer*, *Adv. Energy Mater.* **2** (2012) 1433.

[11] S.M. Abdullah et al., *Modified photo-current response of an organic photodiode by using V2O5 in both hole and electron transport layers*, *Sens. Actuators* **A 272** (2018) 334.

[12] F. Wu et al., *Efficient small-molecule non-fullerene electron transporting materials for high-performance inverted perovskite solar cells*, *J. Mater. Chem.* **A 6** (2018) 4443.

[13] H. Seon et al., *Improvement of the sensitivity of organic polymer-based photodetector fabricated with p-type conjugated polymers for indirect X-ray detection*, 2018 *JINST* **13** C11009.

[14] S.A. Moiz et al., *Space charge-limited current model for polymers*, *Conducting Polymers* (2016) 91.

2020 JINST 15 P02002